


## Article

# Facile Fabrication of Superhydrophobic Graphene/Polystyrene Foams for Efficient and Continuous Separation of Immiscible and Emulsified Oil/Water Mixtures

Chunxia Zhao <sup>1,2,\*</sup> , Haoran Huang <sup>1</sup>, Jiabin Li <sup>1</sup>, Yuntao Li <sup>1,3,\*</sup>, Dong Xiang <sup>1,2</sup>, Yuanpeng Wu <sup>1,2,3</sup> , Ge Wang <sup>1</sup> and Mingwang Qin <sup>4</sup>

<sup>1</sup> School of New Energy and Materials, Southwest Petroleum University, Chengdu 610500, China; HuangHaoran0805@163.com (H.H.); ljx991022@sina.com (J.L.); dxiang01@hotmail.com (D.X.); ypwu@swpu.edu.cn (Y.W.); wangge12335@126.com (G.W.)

<sup>2</sup> The Center of Functional Materials for Working Fluids of Oil and Gas Field, Sichuan Engineering Technology Research Center of Basalt Fiber Composites Development and Application, Southwest Petroleum University, Chengdu 610500, China

<sup>3</sup> State Key Laboratory of Oil and Gas Reservoir Geology and Exploitation, Southwest Petroleum University, Chengdu 610500, China

<sup>4</sup> School of Engineering, Southwest Petroleum University, Nanchong 637001, China; QinMingwang123@126.com

\* Correspondence: polychem2011@hotmail.com (C.Z.); yuntaoli@swpu.edu.cn (Y.L.)



**Citation:** Zhao, C.; Huang, H.; Li, J.; Li, Y.; Xiang, D.; Wu, Y.; Wang, G.; Qin, M. Facile Fabrication of Superhydrophobic Graphene/Polystyrene Foams for Efficient and Continuous Separation of Immiscible and Emulsified Oil/Water Mixtures. *Polymers* **2022**, *14*, 2289. <https://doi.org/10.3390/polym14112289>

Academic Editor: Jin-Hae Chang

Received: 25 April 2022

Accepted: 2 June 2022

Published: 5 June 2022

**Publisher's Note:** MDPI stays neutral with regard to jurisdictional claims in published maps and institutional affiliations.



**Copyright:** © 2022 by the authors. Licensee MDPI, Basel, Switzerland. This article is an open access article distributed under the terms and conditions of the Creative Commons Attribution (CC BY) license (<https://creativecommons.org/licenses/by/4.0/>).

**Abstract:** Three-dimensional superhydrophobic/superlipophilic porous materials have attracted widespread attention for use in the separation of oil/water mixtures. However, a simple strategy to prepare superhydrophobic porous materials capable of efficient and continuous separation of immiscible and emulsified oil/water mixtures has not yet been realized. Herein, a superhydrophobic graphene/polystyrene composite material with a micro-nanopore structure was prepared by a single-step reaction through high internal phase emulsion polymerization. Graphene was introduced into the polystyrene-based porous materials to not only enhance the flexibility of the matrix, but also increase the overall hydrophobicity of the composite materials. The resulting as-prepared monoliths had excellent mechanical properties, were superhydrophobic/superoleophilic (water/oil contact angles were 151° and 0°, respectively), and could be used to continuously separate immiscible oil/water mixtures with a separation efficiency that exceeded 99.6%. Due to the size-dependent filtration and the tortuous and lengthy micro-nano permeation paths, our foams were also able to separate surfactant-stabilized water-in-oil microemulsions. This work demonstrates a facile strategy for preparing superhydrophobic foams for the efficient and continuous separation of immiscible and emulsified oil/water mixtures, and the resulting materials have highly promising application potentials in large-scale oily wastewater treatment.

**Keywords:** graphene; polystyrene; superhydrophobic; porous materials; oily wastewater treatment

## 1. Introduction

Treatment of oily wastewater has attracted growing attention from the academic and industrial sectors in recent years due to the growing global environmental hazards associated with the discharge of industrial and domestic sewage as well as oil spills [1,2]. Traditional disposal techniques used to treat oily wastewater, such as gravity-driven separation, oil skimmers, in situ burning, methods that rely on centrifugal separation, dispersion with chemical reagents and microbial treatments, have low efficiencies, high costs and can even cause secondary pollution to the environment [3–5]. Moreover, treatment of oily wastewater composed of surfactant-stabilized emulsions is even more challenging [6–10]. Therefore, novel techniques and materials that efficiently separate immiscible and emulsified oil/water mixtures are needed for practical use in wastewater treatment.

The high porosity, interconnected pore structure and unique wettability of porous materials make them highly valued in oily wastewater treatment [11,12]. Moreover, the surface wettability of porous materials can be adjusted to tune their selectivity and separation ability for oil/water mixtures [13–20]. For example, Li et al. [21] modified  $\text{Fe}_3\text{O}_4$  nanoparticles with siloxanes and then used the modified nanoparticles to adjust the hydrophobicity of polyurethane foams by a simple drop-coating method. The resulting magnetic materials were able to remotely magnetically absorb oil from water and achieve gravity-driven oil/water separation. Kang et al. [22] prepared a superhydrophobic/superoleophilic material based on the surface modification of wood fibers that showed excellent performance in oil/water separations. Moreover, the prepared material could be used in multiple environments and achieved highly efficient absorption- and filtration-based separation of oil/water mixtures. While these materials were able to absorb oil from wastewater, treating large-scale oil spills with such types of oil sorbents is a time-consuming and labor-intensive task. A large amount of absorbent material is often required because the absorbents have a limited capacity for the oils [23]. Moreover, absorbent-based separations are not scalable for large-scale oily wastewater treatment because the oil/water mixtures must be collected before it can be filtered [24–27]. Therefore, in order to simplify the separation process, it is necessary to design and manufacture devices based on oil absorbing materials that can continuously and efficiently handle oily wastewater. Towards this goal, Ge et al. developed an in situ oil collection device that was aided by the application of external force [28]. Such continuous oil collection processes require oil absorbing materials with high mechanical performances as well as excellent hydrophobic and lipophilic properties [29]. Many strategies have been developed for the modification of commercial melamine foams, polyurethane foams or metal foams (pore sizes ranging from 100 to 500  $\mu\text{m}$ ) to create materials with the desired characteristics for the continuous clean-up of large-scale oil spills [22,30–32]. Although the design of these superwetting foams is exquisite, the pore structure of the matrix material is not sufficient to act as particle sieves and separate emulsions, especially emulsions with particle sizes less than 20  $\mu\text{m}$  [33–35]. On the other hand, the surface modification of the matrix material requires either complicated procedures or expensive equipment, and even fluorochemicals are utilized to reduce the surface energy, causing secondary environmental pollution. Therefore, the exploration of new strategies for the preparation of superwetable materials with controlled pore structures is needed to realize the continuous and efficient separation of immiscible and emulsified oil/water mixtures.

In recent years, the high internal phase emulsion (HIPE) templating method has been studied extensively to prepare polymer-based porous materials with adjustable pore structures and porosities [36–43]. However, the HIPE templating method is typically performed using rigid monomers, and the resulting porous materials have poor mechanical properties in that they are highly brittle and easily pulverized [44,45]. In addition, the hydrophobic properties of such materials need to be further improved for practical applications in handling oily wastewater [46]. To address these limitations, here we prepare graphene/polystyrene (GN/PSt) porous materials via the HIPE templating method. The introduction of graphene simultaneously improves the flexibility and enhances the hydrophobic properties of the polymer-based matrix. The as-prepared GN<sub>4</sub>/PSt superhydrophobic porous materials achieved in situ continuous absorption of heavy and light oils from water with separation efficiencies that exceeded 99.6%. Moreover, the micro-nanopore structure and wettability of the prepared materials allowed for the efficient and continuous separation of surfactant-stabilized water-in-oil microemulsions. These advantages demonstrate the potential value of our prepared foams for the large-scale and continuous separation of immiscible and emulsified oil/water mixtures.

## 2. Materials and Methods

### 2.1. Materials

Styrene (St) and Span 80 were obtained from Innochem Technology Co., Ltd., Beijing, China. Divinylbenzene (DVB), sodium persulfate ( $\text{Na}_2\text{S}_2\text{O}_8$ ) and sodium dodecyl

sulfonate (SDS) were obtained from Aldrich, Shanghai, China. Graphene (GN, lamellae size 5–15  $\mu\text{m}$ ) was supplied by Deyang Carbonene Technology Co., Ltd. (Deyang, China), and the lamellae were composed of five to six layers of graphene. Absolute ethanol, petroleum ether, chloroform, toluene and acetone were all purchased from Chengdu Kelong Chemical Reagent Factory. Ultrapure deionized water from an ultrapure water machine was used to prepare all solutions.

## 2.2. Fabrication of GN/PSt Foams

In a typical preparation process, 0.02 g of  $\text{Na}_2\text{S}_2\text{O}_8$ , 0.004 g of SDS and 0.02 g of GN were ultrasonically dispersed in 20 mL deionized water to obtain a homogeneous solution. This solution was then gradually added to a beaker containing 0.3 g of St, 0.2 g of DVB and 0.15 g of Span 80, and the mixture was stirred at 200 rpm until a homogeneous and viscous solution was formed, which was the HIPE pre-polymerization mixture. The beaker was sealed and kept at 65 °C for 8 h to allow the polymerization reaction to proceed. After polymerization, the product was washed with absolute ethanol to remove the Span 80 and unreacted organic monomers. The obtained gray monolith was dried at 50 °C for 10 h in a blast oven. The prepared superhydrophobic polystyrene-based porous material containing 4 wt% GN was labeled as  $\text{GN}_4/\text{PSt}$ . Samples containing 0 wt%, 2 wt%, 8 wt% and 10 wt% GN were prepared following the same protocol and were labelled as  $\text{GN}_0/\text{PSt}$ ,  $\text{GN}_2/\text{PSt}$ ,  $\text{GN}_8/\text{PSt}$  and  $\text{GN}_{10}/\text{PSt}$ , respectively. The fabrication process is schematically illustrated in Figure 1.

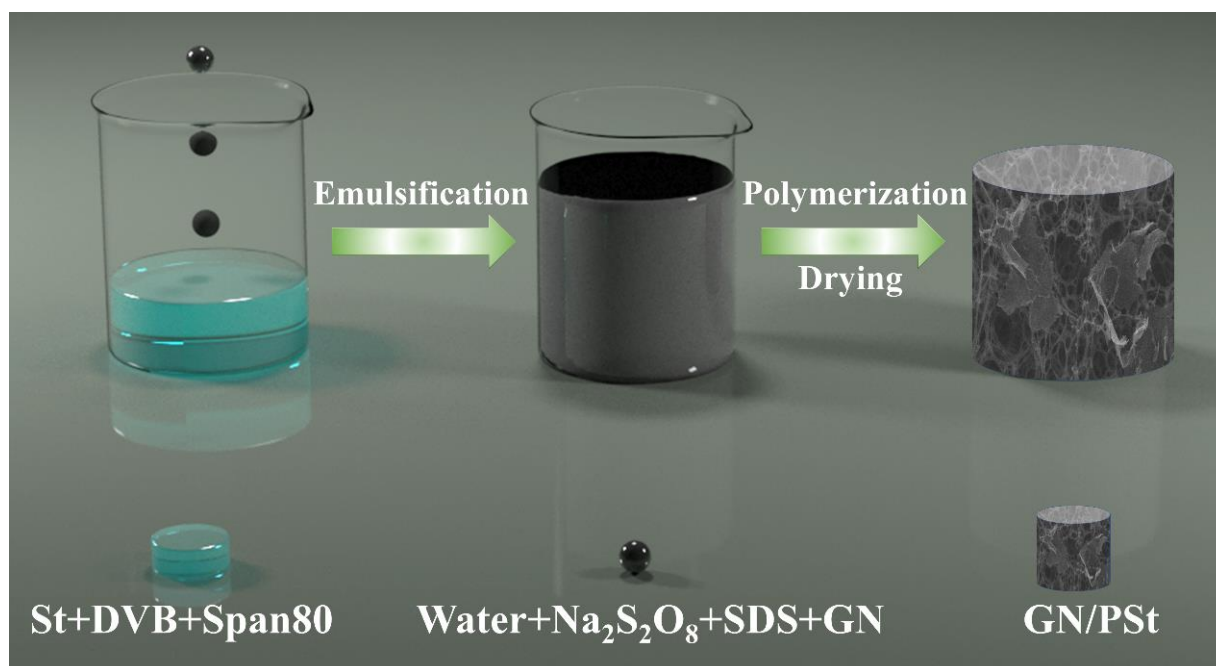


**Figure 1.** Schematic illustration of the fabrication of superhydrophobic GN/PSt foams.

## 2.3. Characterization

The microscopic pore structures in the prepared materials were characterized with scanning electron microscopy (SEM, JEOL JSM-5009LV), and the pore size distribution and porosity of the  $\text{GN}_4/\text{PSt}$  composites were determined using an automatic mercury porosimeter (Mike 9500). The water contact angles (WCA), rolling angles (RA) and oil contact angles (OCA) were characterized using a contact angle goniometer (OCA 25, Data physics Instruments GmbH, Filderstadt, Germany). Contact angle measurements were made by dropping 3  $\mu\text{L}$  of deionized water or petroleum ether on three different locations of each sample surface, and the average value is presented. The compressive properties of the porous materials were evaluated using a universal material testing machine (CMT4104,

MTS, USA) with a compression rate of 2 mm/min. Samples used in the compressive tests were cylindrical with a height of  $20 \pm 2$  mm and a diameter of 24 mm.

### 2.3.1. Oil Absorption Capacity

The saturated oil absorption capacity ( $k$ ) of the GN<sub>4</sub>/PSt superhydrophobic porous material was calculated according to Equation (1) [12]:

$$k = \frac{m_1 - m_0}{m_0} \quad (1)$$

where  $m_0$  is the original mass of the GN<sub>4</sub>/PSt porous material, and  $m_1$  is the mass of the GN<sub>4</sub>/PSt porous material saturated with oil.

### 2.3.2. Oil/Water Mixture Separation Efficiency

The model oil/water mixtures were continuously separated using the prepared porous materials with the aid of an external pump, and the separation efficiency ( $\eta$ ) was calculated following Equation (2):

$$\eta = \frac{m_a}{m_b} \times 100\% \quad (2)$$

where  $m_b$  and  $m_a$  denoted the water mass before and after separation, respectively.

### 2.3.3. Emulsified Oil/Water Mixture Separation Experiments

Three surfactant-stabilized water-in-oil (W/O) emulsions (water/petroleum ether; water/toluene; water/chloroform) were prepared to simulate stable oil/water mixtures found in real world applications. The emulsions were prepared by mixing water and oil ( $V_{\text{water}}:V_{\text{oil}} = 1:100$ ) with 1 g/L Span 80 under vigorous stirring for 1 h. The resulting emulsions were stable for at least 24 h.

Continuous oil/water emulsion separation experiments were performed with the aid of an external power source. Microscopic images of the emulsions before and after separation with the GN/PSt composites were taken with an eyepiece inverted fluorescent digital microscope (AMG EVOSFL, USA).

The separation efficiency ( $E$ ) of the oil/water emulsion was calculated according to Equation (3) [47]:

$$E = \left(1 - \frac{C_s}{C_0}\right) \times 100\% \quad (3)$$

where  $C_0$  and  $C_s$  represent the moisture content in the emulsion and the filtrate, respectively, and the moisture contents in the oil were determined using a Karl Fischer moisture meter (Mettler V10S).

## 3. Results and Discussion

### 3.1. Characterizations of the GN/PSt Composites

During HIPE, water was dispersed in an organic continuous phase consisting of St and DVB, forming a water-in-oil emulsion stabilized by the lipophilic surfactant, Span 80, co-Pickering-surfactant and GN nanosheets. The organic phase, St and DVB, was then polymerized to form the skeleton of the porous material [48], and the water phase was removed from the pore cavities to give the GN/PSt porous materials with high porosities and open pore structures (Figure 2). As seen in the SEM images in Figure 2a, the GN/PSt composites contained interconnected polymer walls that formed large spherical pores (Figure 2a), and many smaller pores were present within the polymer skeleton (Figure 2b) [49]. GN randomly penetrated into the matrix of the porous materials, resulting in a rougher microstructure and lower surface energy (Figure 2c–f) [50]. Similar interconnected porous structures were seen in the GN<sub>0</sub>/PSt, GN<sub>2</sub>/PSt and GN<sub>4</sub>/PSt composites, which should be advantageous for the better transfer of substances through the porous materials when the monoliths are used to separate oil/water mixtures. Meanwhile, a more closed-cell structure



was seen in the GN/PSt composites prepared with 8% and 10% GN (Figure 2g–j) because the GN agglomerated and was harder to disperse at these high concentrations and such a closed cell structure is not conducive to the transfer of matter through the materials.

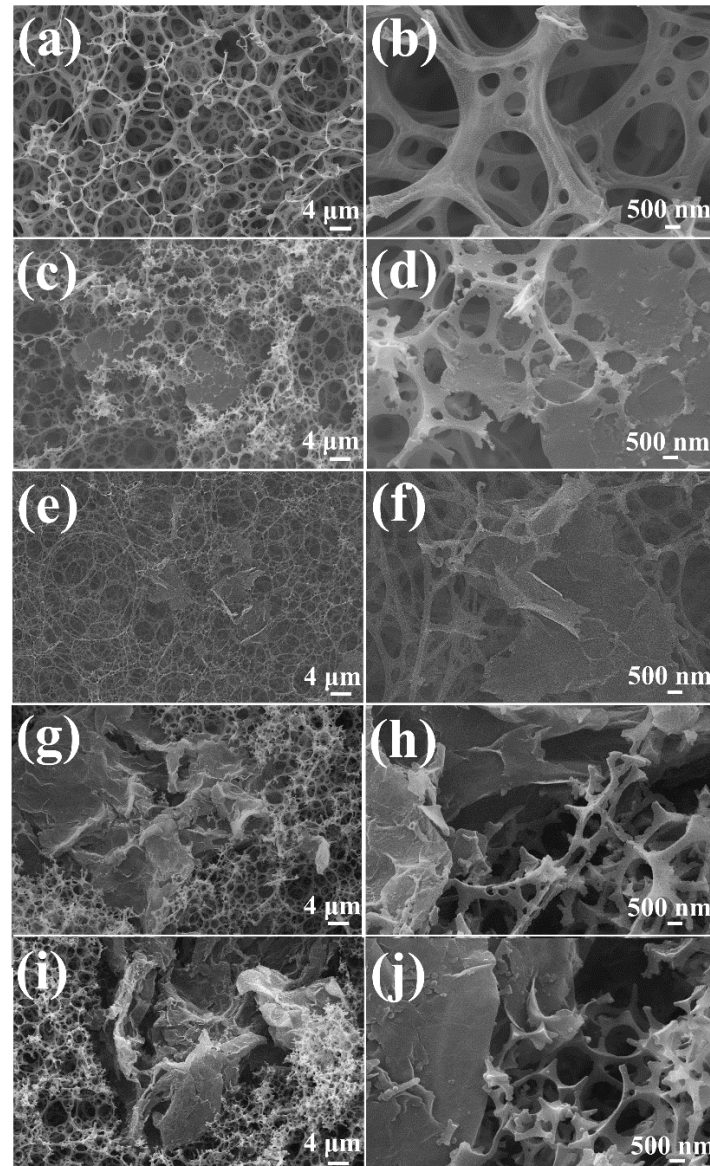


**Figure 2.** SEM images of the GN<sub>0</sub>/PSt (a,b), GN<sub>2</sub>/PSt (c,d), GN<sub>4</sub>/PSt (e,f), GN<sub>8</sub>/PSt (g,h) and GN<sub>10</sub>/PSt (i,j) composites.

Moreover, the Raman spectra of GN and the GN<sub>4</sub>/PSt composite are shown in Figure S1. Two obvious peaks corresponding to D and G bands appeared at approximately  $1358\text{ cm}^{-1}$  and  $1586\text{ cm}^{-1}$ , respectively. The G band was generally associated with the  $E_{2g}$  phonon of the C  $sp^2$  atom, while the D band arose from the activation of the first-order scattering process of the  $sp^3$  carbon atom in graphene sheets [51]. In the GN<sub>4</sub>/PSt composite, the same characteristic peaks as GN clearly appeared. This result demonstrated that the composite was successfully prepared. Furthermore, the intensity ratio of D bands to G bands (ID/IG) is usually adopted to evaluate the defects of graphene sheets. The ID/IG of GN used in this experiment was approximately 0.1071, and it increased substantially to 0.1897 for the GN<sub>4</sub>/PSt composite. The higher ID/IG of GN<sub>4</sub>/PSt resulted from a decrease in the crystalline  $sp^2$  domains of GN, which may be caused by the intercalation of monomer polymerization in the GN layers [52].

### 3.2. Hydrophobicity of the GN/PSt Composites

The wettability of the GN/PSt porous materials was quantified by their water contact angles. As shown in Figure 3, the WCA of the GN/PSt composite foams was higher than that of the pure foam prepared without GN or GN<sub>0</sub>/PSt (WCA— $140.5 \pm 0.7^\circ$ ), suggesting that the addition of the GN nanosheets made the PSt-based foams more hydrophobic. The highest WCA was measured for the GN<sub>4</sub>/PSt composite monolith (WCA— $150.9 \pm 0.6^\circ$ ), indicating that it was the most hydrophobic of the prepared materials.

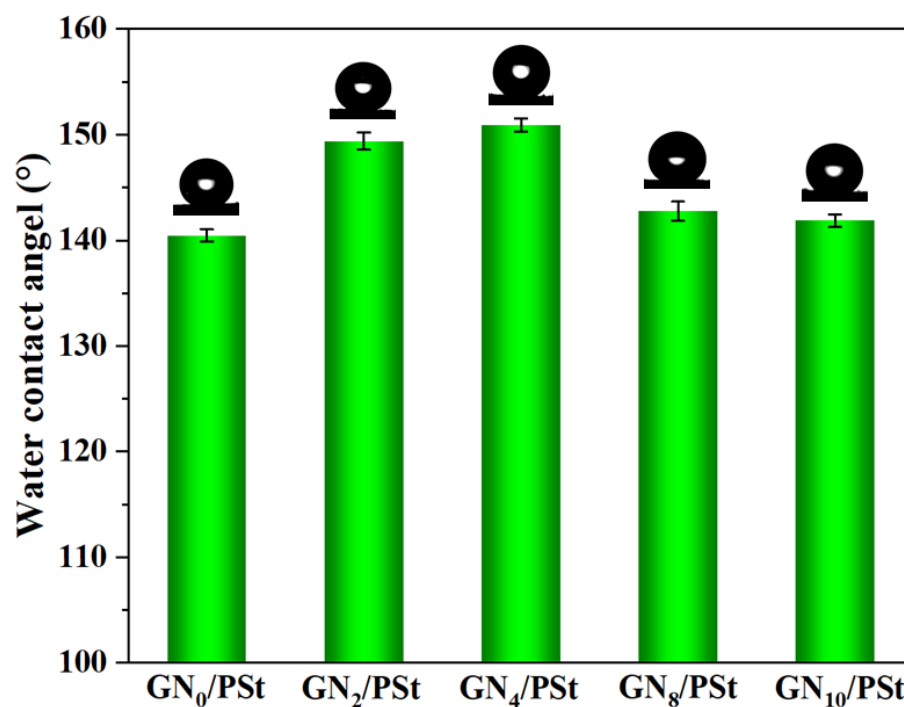


Figure 3. WCAs of the GN/PSt composite porous materials.

### 3.3. Mechanical Properties of GN/PSt Composites

To be useful in practical applications, the porous material used for oil/water separation processes must have excellent mechanical properties [53]. Figure 4 shows that the overall trends in the compressive stress–strain curves measured for the GN/PSt composites with different GN contents were similar, and the curves could be divided into three stages. At strains less than 10%, the stress increased linearly with the applied strain. Between 10% and 60% strain, the measured stress plateaued, indicating that the porous material absorbed a large amount of compressive energy and suggesting that the skeleton of the structure was highly deformed. At strains greater than 60%, the material began to fracture under the applied pressure and underwent a densification process. At this time, the stress increased sharply with the increase in the strain [54]. Materials prepared by HIPE polymerization have poor mechanical properties, for example, they are highly brittle and easily pulverized, due to the use of rigid monomers and the high crosslinking densities of the final materials [44]. Here, we see that as the amount of GN added during the HIPE polymerization increased, the compressive strength of the resulting composite materials first decreased and then increased. Small amounts of added GN increased the flexibility of the material, but the addition of excessive amounts of GN resulted in uneven dispersion and agglomeration of the nanosheets, which concentrated the stress and reduced the flexibility of the final composite material. From the present studies, the addition of 4% GN was the optimal amount to effectively improve the flexibility of the porous material while also increasing its hydrophobicity. Therefore, GN<sub>4</sub>/PSt was selected for the subsequent tests.

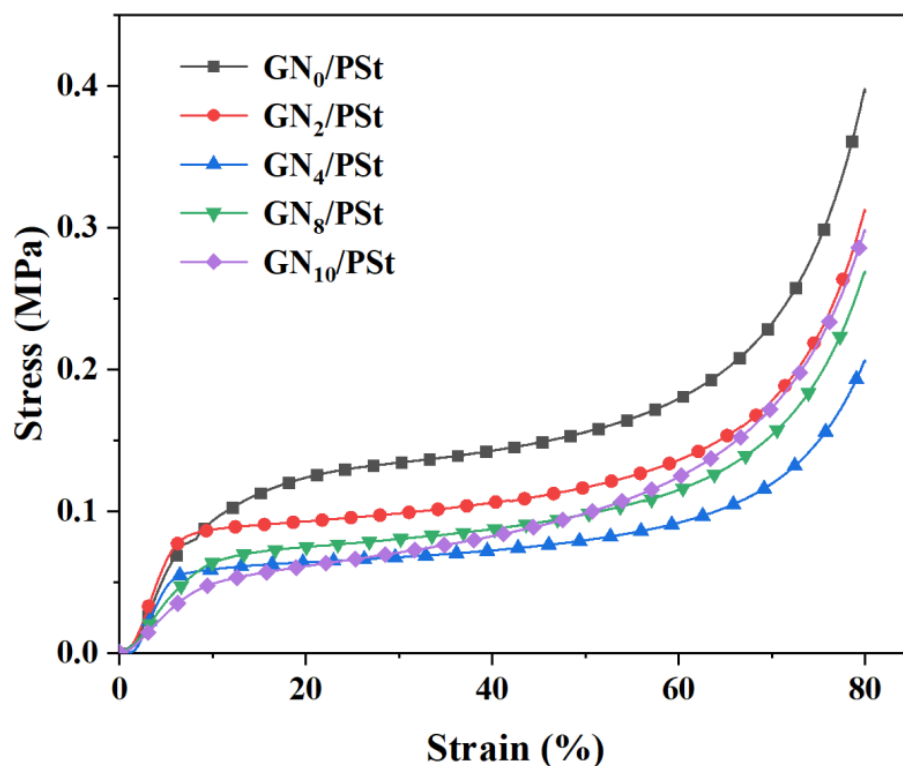
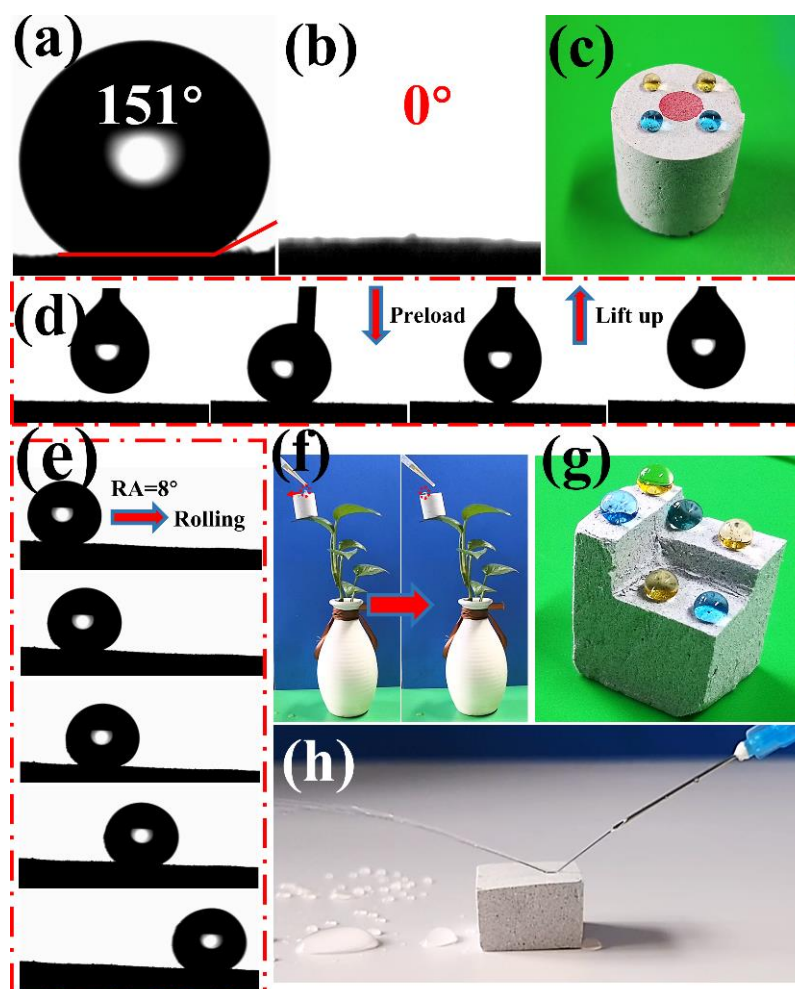


Figure 4. Compressive stress–strain curve measured of the composite porous materials.

### 3.4. Wettability of GN<sub>4</sub>/PSt Composites

The wettability of porous materials towards water and oil is a vital indicator of their performance in oil/water separations [55]. As seen in Figure 5a,b, the WCA and OCA of the GN<sub>4</sub>/PSt porous composite were 151° and 0°, respectively. To more clearly demonstrate the superhydrophobicity and oleophilicity of the prepared composite, water and oil were dropped onto the surface of the GN<sub>4</sub>/PSt monolith, and the water droplets remained as spherical shapes while the oil droplets were rapidly absorbed (Figure 5c). Under the application of an external force, a water droplet was forced to make contact and move on the surface of the material, and the water droplet moved easily and did not remain on the surface of the foam, suggesting that the water adhesion on the GN<sub>4</sub>/PSt composite was extremely low (Figure 5d). Moreover, the rolling angle (RA) of the material was small (RA = 8°, Figure 5e). As shown in Figure 5f, the lightweight GN<sub>4</sub>/PSt porous material could be placed on a thin blade, and a water droplet placed on the surface easily rolled off at only a slight incline due to the low density and low RA of the prepared composite materials. An automatic mercury porosimeter was used to characterize the pore structure of GN<sub>4</sub>/PSt composites, and the density and porosity were 0.0276 g/cm<sup>3</sup> and 97.2%, respectively. The results indicated that the GN<sub>4</sub>/PSt foam had a hierarchical pore structure containing both nanopores (40–1000 nm) and micropores (1–20 μm) (ESI; Figure S2), suggesting that the prepared material should be able to separate oil/water emulsions through a size sieving effect [56]. Moreover, the properties of the GN<sub>4</sub>/PSt porous sample were highly uniform, and the monolith could be randomly cut into various segments without affecting the shapes of the water droplets on any of the surfaces (Figure 5g). Figure 5h shows that the GN<sub>4</sub>/PSt porous material also had a strong water-impact resistance [57]. In summary, the addition of GN into an HIPE system resulted in GN<sub>4</sub>/PSt composite materials with superhydrophobic/superoleophilic properties as well as a low density and high porosity, making this material especially promising for the purification of oily sewage.



**Figure 5.** (a) WCA and (b) OCA of GN<sub>4</sub>/PSt, (c) photographs of water (dyed with brilliant green and methyl orange) and oil (dyed with oil red O) droplets on the surface of GN<sub>4</sub>/PSt, (d) dynamic adhesion behavior of water droplets on GN<sub>4</sub>/PSt surface, (e) the rolling angle, (f) water droplets falling on the surface of GN<sub>4</sub>/PSt, (g) water droplets on a random surface of GN<sub>4</sub>/PSt, (h) water impact resistance of GN<sub>4</sub>/PSt.

### 3.5. Oil Absorption Capacity and Continuous Oil/Water Separation Using the GN<sub>4</sub>/PSt Composites

As shown in Figure 6a,b, both light (petroleum ether) and heavy (chloroform) oils were rapidly absorbed into the GN<sub>4</sub>/PSt composite by capillary forces, suggesting the prepared composites should show good performance in water/oil separation experiments. The saturated oil absorption capacity of the GN<sub>4</sub>/PSt foams for various types of organic solvents (Figure 6c) and ranged from 27.44 to 56.9 g/g. These results suggested that the prepared composites had a high absorption capacity for various organic solvents, and the variations in the different oil absorption capacities were due to differences in the densities and viscosities of the absorbed organic solvents [58]. The reusability of materials is also a key factor in the actual treatment of oily wastewater. The reusability of GN<sub>4</sub>/PSt foam was examined by absorption-centrifugation. After the oil absorption reached saturation, the oil in the GN<sub>4</sub>/PSt foam was removed by centrifugation at 6000 rpm for 2 min, while the foam was regenerated for the next absorption/centrifugation cycle without further treatment (Figure S3a). The absorption/centrifugation cycle test was repeated 10 times and the results are shown in Figure S3b. The porous material exhibited stable reuse performance with almost no change in oil absorption capacity, and approximately 84% of petroleum ether was removed by each centrifugation. It is speculated that the residual petroleum ether was



stably adsorbed and retained in the micropores by van der Waals and capillary forces. In addition, the GN<sub>4</sub>/PSt sample continuously absorb oil pumped through the foam, which is a necessary feature of materials used in large-scale oily wastewater treatment. As shown in Figure 6d and Video S1, both light oil (petroleum ether) and heavy oil (chloroform) were quickly and continuously separated from water without leaving any residual red oil in the water phase. As shown in Figure 6e, the GN<sub>4</sub>/PSt foams maintained a high separation efficiency for various organic solvents in water (above 99.6%), further highlighting that the GN<sub>4</sub>/PSt composite material has great application potential for efficient, large-scale and continuous treatment of oily wastewater.

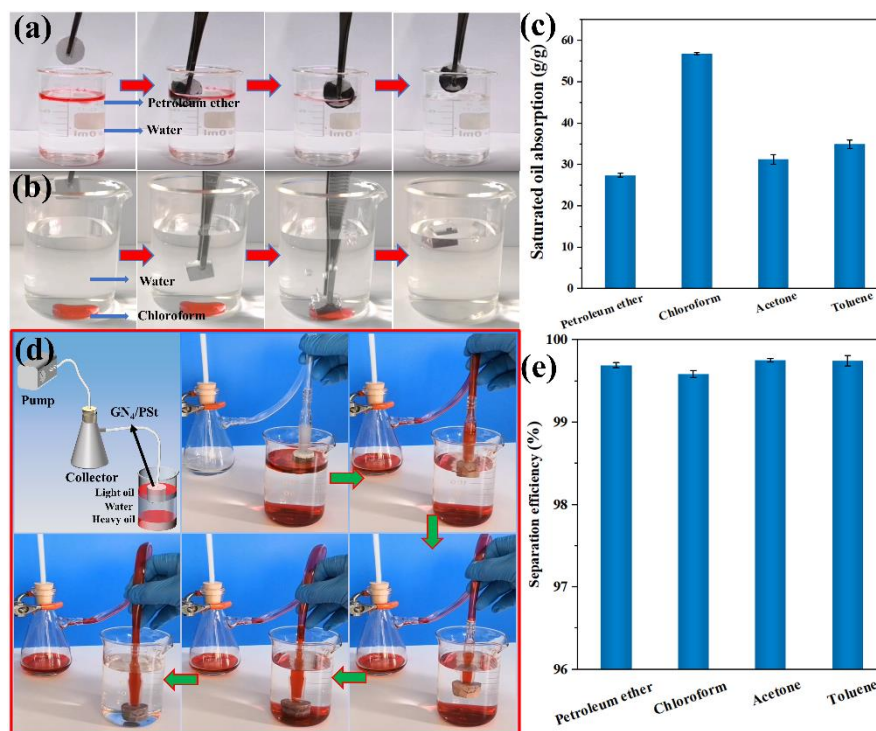


**Figure 6.** Photographs showing the use of GN<sub>4</sub>/PSt composite materials for selective oil/water separation. (a) Petroleum ether/water and (b) chloroform/water, (c) the saturated oil absorption capacity of GN<sub>4</sub>/PSt foam for a variety of organic solvents, (d) images of the continuous separation of light oil/water/heavy oil mixtures using the GN<sub>4</sub>/PSt foams and corresponding (e) separation efficiencies for different oil/water mixtures.

### 3.6. Continuous Separation of Surfactant-Stabilized Emulsions Using the GN<sub>4</sub>/PSt Composites

The separation of emulsions is much more difficult than the separation of immiscible water/oil mixtures, and the separation of surfactant-stabilized microemulsions with small droplet sizes and lower content of dispersive phase is especially challenging [59]. To test the feasibility of separating oil/water emulsions using the GN<sub>4</sub>/PSt foams, three surfactant-stabilized water-in-oil emulsions with micro-nano particle sizes were prepared, and the separation of Span 80-stabilized water-in-petroleum ether emulsions are discussed as an example. As shown in Figure 7a and Video S2, after the milky white emulsion was pumped through the monolith, the filtrate was clear and transparent indicating that in situ demulsification and continuous oil/water separation were realized. Moreover, optical micrographs and digital photographs of the as-prepared water-in-oil emulsions before and after separation using the GN<sub>4</sub>/PSt foams are shown in Figure 7b–d. While numerous dispersed droplets were seen in the feed solutions, no droplets were observed in the filtrate using an optical microscope, further highlighting the high-efficiency separation performance of the GN<sub>4</sub>/PSt foams. Furthermore, the droplet size of the feed emulsions and filtrates were measured using the dynamic light scattering. The initial emulsions

contained a wide size distribution of droplets ranging from 30 nm to 7  $\mu\text{m}$  (Figure 7e). In comparison, the droplets in the filtrate were smaller than 100 nm (Figure 7f), and the particle sizes were similar to those seen in a solution of the Span 80 surfactant in oil (Figure 7g). Based on these results, we speculate that the filtrate was composed of a small number of nano-sized emulsified water droplets and surfactant micelles [56,60].

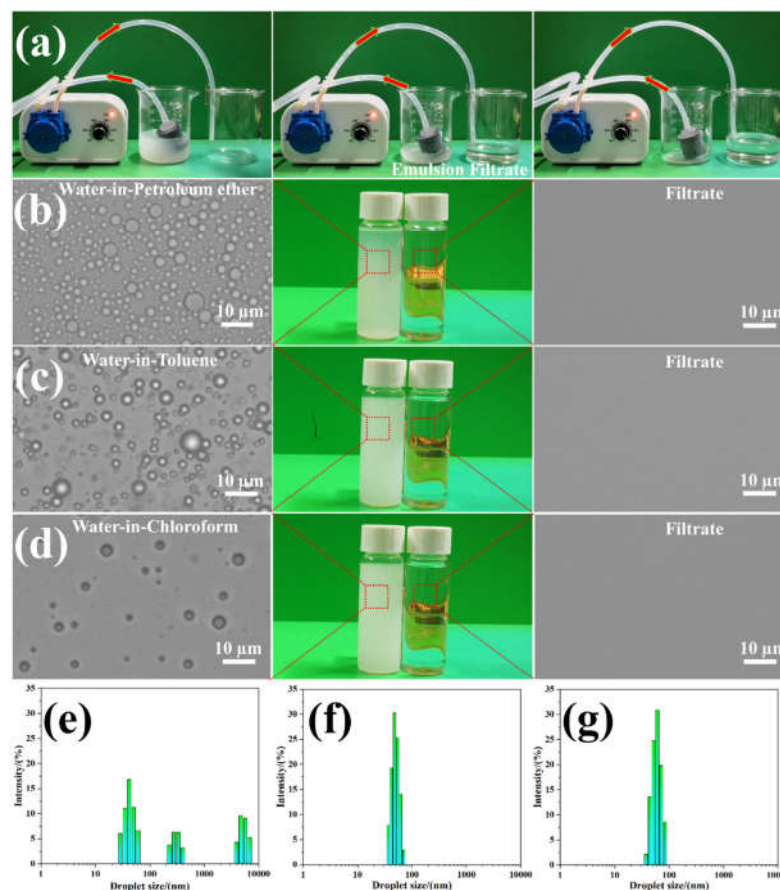


**Figure 7.** (a) Photographs of the setup using GN<sub>4</sub>/PSt composites for the continuous separation of water-in-petroleum ether emulsions and corresponding optical microscopy images and digital photos of the emulsions before and after separation, (b) water-in-petroleum ether emulsions, (c) water-in-toluene emulsions, (d) water-in-chloroform emulsions, (e) droplet size distributions in the water-in-petroleum ether emulsion, (f) droplet size distribution in the filtrate, and (g) droplet size distribution in a solution of 1 g/L Span 80 surfactant in petroleum ether.

To more quantitatively assess the demulsification efficiency of the GN<sub>4</sub>/PSt foams, the moisture contents of the emulsions before and after the separation were measured using a Karl Fischer moisture meter, and the results are shown in Figure 8. The separation efficiencies of the GN<sub>4</sub>/PSt composites for the three emulsions were 98.2%, 98.5% and 98.2%, respectively. This high separation efficiency is due to a combination of size-sieving filtration in the GN<sub>4</sub>/PSt foams as well as the completely opposite wettability towards oil and water. The long and tortuous micro-nano permeation channels in the foams were also crucial in the emulsion separation process [35,61,62]. In summary, the as-prepared superhydrophobic GN<sub>4</sub>/PSt porous materials could be used for the efficient, large-scale and continuous separation of emulsions to achieve rapid treatment of emulsified oily sewage.

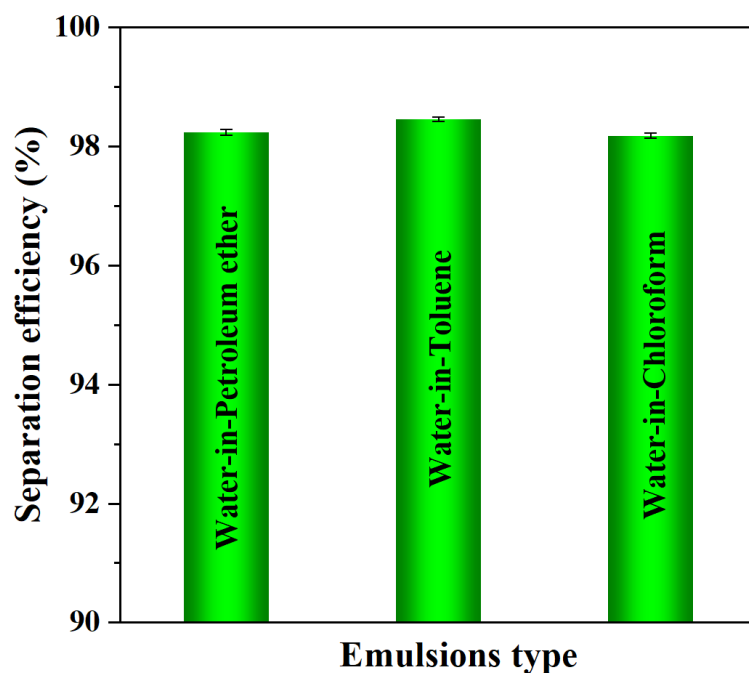


Figure 8. Separation efficiency of water-in-oil emulsions.

#### 4. Conclusions

In summary, the superhydrophobic GN<sub>4</sub>/PSt composite material with micro-nanopore structures was successfully fabricated using a facile, low-cost HIPE polymerization method. Compared with a neat porous material prepared with only PSt, the porous monolith prepared with 4 wt% GN was more hydrophobic (WCA increased from  $140.5 \pm 0.7^\circ$  to  $150.9 \pm 0.6^\circ$ ) and more flexible. Due to the ideal wettability, excellent mechanical properties and high porosity (97.2%), the GN<sub>4</sub>/PSt composite monolith could be used to continuously separate immiscible oil/water mixtures with a separation efficiency above 99.6%. Arising from the lengthy micro-nanopore permeation path, the GN<sub>4</sub>/PSt enable efficient and continuous separation of surfactant-stabilized water-in-oil microemulsions. The special wettability, hierarchical pore structure with micro-nanopore and tortuous permeation channel play the significant roles in emulsion separation. The superhydrophobic GN<sub>4</sub>/PSt composite material prepared here showed great performance for the efficient and continuous separation of immiscible and emulsified oil/water mixtures and has promising application prospects in the practical large-scale treatment of oily wastewater.

**Supplementary Materials:** The following supporting information can be downloaded at: <https://www.mdpi.com/article/10.3390/polym14112289/s1>, Figure S1. Raman spectra of GN and GN<sub>4</sub>/PSt.; Figure S2. The pore size distribution of GN<sub>4</sub>/PSt porous material.; Figure S3. (a) The process of removal of petroleum ether from oil/water mixture and the regeneration of the foam. (b) Regeneration of GN<sub>4</sub>/PSt sponge during the absorption of petroleum ether for 10 cycles.; Video 1: Continuous separation of immiscible light oil/water/heavy oil by GN<sub>4</sub>/PSt porous material with the assistance of a pump.; Video 2: Continuous separation of surfactant-stabilized water-in-oil microemulsions with the assistance of a pump.

**Author Contributions:** Conceptualization, C.Z. and Y.L.; methodology, H.H.; software, D.X. and Y.W.; validation, H.H. and J.L.; formal analysis, H.H., D.X. and Y.W.; investigation, H.H.; resources, C.Z. and M.Q.; data curation, H.H.; writing—original draft preparation, H.H.; writing—review and editing, C.Z. and Y.L.; visualization, H.H. and G.W.; supervision, C.Z. and Y.L.; project administration, C.Z., H.H. and Y.L.; funding acquisition, C.Z. and M.Q. All authors have read and agreed to the published version of the manuscript.

**Funding:** This work was supported by the Science and Technology Strategic Cooperation Special Project of Nanchong City and SWPU (SXHZ046), and the Innovation and Entrepreneurship Training Program for College Students of Sichuan Province (S202110615095).

**Institutional Review Board Statement:** Not applicable.

**Informed Consent Statement:** Not applicable.

**Data Availability Statement:** Not applicable.

**Conflicts of Interest:** The authors declare no conflict of interest.

## References

1. Almeda, R.; Wambaugh, Z.; Wang, Z.; Hyatt, C.; Liu, Z.; Buskey, E.J. Interactions between Zooplankton and Crude Oil: Toxic Effects and Bioaccumulation of Polycyclic Aromatic Hydrocarbons. *PLoS ONE* **2013**, *8*, e67212. [[CrossRef](#)]
2. Peterson, C.H.; Rice, S.D.; Short, J.W.; Esler, D.; Bodkin, J.L.; Ballachey, B.E.; Irons, D.B. Long-Term Ecosystem Response to the Exxon Valdez Oil Spill. *Science* **2003**, *302*, 2082–2086. [[CrossRef](#)]
3. Jamaly, S.; Giwa, A.; Hasan, S.W. Recent Improvements in Oily Wastewater Treatment: Progress, Challenges, and Future Opportunities. *J. Environ. Sci.* **2015**, *37*, 15–30. [[CrossRef](#)]
4. Ezzat, A.O.; Atta, A.M.; Al-Lohedan, H.A. One-Step Synthesis of Amphiphilic Nonylphenol Polyethyleneimine for Demulsification of Water in Heavy Crude Oil Emulsions. *ACS Omega* **2020**, *5*, 9212–9223. [[CrossRef](#)]
5. Ye, F.; Jiang, X.; Mi, Y.; Kuang, J.; Huang, Z.; Yu, F.; Zhang, Z.; Yuan, H. Preparation of Oxidized Carbon Black Grafted with Nanoscale Silica and Its Demulsification Performance in Water-in-Oil Emulsion. *Colloids Surfaces A Physicochem. Eng. Asp.* **2019**, *582*, 123878. [[CrossRef](#)]
6. Zhu, Y.; Wang, D.; Jiang, L.; Jin, J. Recent Progress in Developing Advanced Membranes for Emulsified Oil/Water Separation. *NPG Asia Mater.* **2014**, *6*, e101. [[CrossRef](#)]
7. Xu, L.; Chen, Y.; Liu, N.; Zhang, W.; Yang, Y.; Cao, Y.; Lin, X.; Wei, Y.; Feng, L. Breathing Demulsification: A Three-Dimensional (3D) Free-Standing Superhydrophilic Sponge. *ACS Appl. Mater. Interfaces* **2015**, *7*, 22264–22271. [[CrossRef](#)]
8. Zulfiqar, U.; Thomas, A.G.; Yearsley, K.; Bolton, L.W.; Matthews, A.; Lewis, D.J. Renewable Adsorbent for the Separation of Surfactant-Stabilized Oil in Water Emulsions Based on Nanostructured Sawdust. *ACS Sustain. Chem. Eng.* **2019**, *7*, 18935–18942. [[CrossRef](#)]
9. Tao, M.; Xue, L.; Liu, F.; Jiang, L. An Intelligent Superwetting PVDF Membrane Showing Switchable Transport Performance for Oil/Water Separation. *Adv. Mater.* **2014**, *26*, 2943–2948. [[CrossRef](#)]
10. Wang, G.; He, Y.; Wang, H.; Zhang, L.; Yu, Q.; Peng, S.; Wu, X.; Ren, T.; Zeng, Z.; Xue, Q. A Cellulose Sponge with Robust Superhydrophilicity and Under-Water Superoleophobicity for Highly Effective Oil/Water Separation. *Green Chem.* **2015**, *17*, 3093–3099. [[CrossRef](#)]
11. Li, X.; Cao, M.; Shan, H.; Tezel, F.H.; Li, B. Facile and Scalable Fabrication of Superhydrophobic and Superoleophilic PDMS-co-PMHS Coating on Porous Substrates for Highly Effective Oil/Water Separation. *Chem. Eng. J.* **2019**, *358*, 1101–1113. [[CrossRef](#)]
12. Liu, S.; Zhang, X.; Seeger, S. Tunable Bulk Material with Robust and Renewable Superhydrophobicity Designed via In-Situ Loading of Surface-Wrinkled Microparticles. *Chem. Eng. J.* **2020**, *408*, 127301. [[CrossRef](#)]
13. Cheng, Z.J.; Zhang, D.J.; Luo, X.; Lai, H.; Liu, Y.Y.; Jiang, L. Superwetting Shape Memory Microstructure: Smart Wetting Control and Practical Application. *Adv. Mater.* **2021**, *33*, 2001718–2001733. [[CrossRef](#)]
14. Du, R.; Zhao, Q.; Zheng, Z.; Hu, W.; Zhang, J. 3D Self-Supporting Porous Magnetic Assemblies for Water Remediation and Beyond. *Adv. Energy Mater.* **2016**, *6*, 1600473. [[CrossRef](#)]
15. Li, L.X.; Zhang, J.P.; Wang, A.Q. Removal of Organic Pollutants from Water Using Superwetting Materials. *Chem. Rec.* **2018**, *18*, 118–136. [[CrossRef](#)]
16. Wang, S.; Liu, K.; Yao, X.; Jiang, L. Bioinspired Surfaces with Superwettability: New Insight on Theory, Design, and Applications. *Chem. Rev.* **2015**, *115*, 8230–8293. [[CrossRef](#)]
17. Zhang, N.; Qi, Y.; Zhang, Y.; Luo, J.; Cui, P.; Jiang, W. A Review on Oil/Water Mixture Separation Material. *Ind. Eng. Chem. Res.* **2020**, *59*, 14546–14568. [[CrossRef](#)]
18. Liu, M.; Wang, S.; Jiang, L. Nature-Inspired Superwettability Systems. *Nat. Rev. Mater.* **2017**, *2*, 17036. [[CrossRef](#)]
19. Shen, L.; Pan, Y.; Fu, H. Fabrication of UV Curable Coating for Super Hydrophobic Cotton Fabrics. *Polym. Eng. Sci.* **2019**, *59*, E452–E459. [[CrossRef](#)]
20. Shan, W.W.; Du, J.; Yang, K.; Ren, T.B.; Wan, D.C.; Pu, H.T. Superhydrophobic and Superoleophilic Polystyrene/Carbon Nanotubes Foam for Oil/Water Separation. *J. Environ. Chem. Eng.* **2021**, *9*, 106038–106046. [[CrossRef](#)]
21. Li, Z.T.; Lin, B.; Jiang, L.W.; Lin, E.C.; Chen, J.; Zhang, S.J.; Tang, Y.W.; He, F.A.; Li, D.H. Effective Preparation of Magnetic Superhydrophobic Fe<sub>3</sub>O<sub>4</sub>/PU Sponge for Oil-Water Separation. *Appl. Surf. Sci.* **2018**, *427*, 56–64. [[CrossRef](#)]
22. Kang, L.; Shi, L.; Zeng, Q.; Liao, B.; Wang, B.; Guo, X. Melamine Resin-Coated Lignocellulose Fibers with Robust Superhydrophobicity for Highly Effective Oil/Water Separation. *Sep. Purif. Technol.* **2021**, *279*, 119737. [[CrossRef](#)]
23. Shang, Q.; Chen, J.; Hu, Y.; Yang, X.; Hu, L.; Liu, C.; Ren, X.; Zhou, Y. Facile Fabrication of Superhydrophobic Cross-Linked Nanocellulose Aerogels for Oil–Water Separation. *Polymers* **2021**, *13*, 625. [[CrossRef](#)]



24. Kong, Z.; Wang, J.; Lu, X.; Zhu, Y.; Jiang, L. In Situ Fastening Graphene Sheets into a Polyurethane Sponge for the Highly Efficient Continuous Cleanup of Oil Spills. *Nano Res.* **2017**, *10*, 1756–1766. [[CrossRef](#)]
25. Gong, Z.; Yang, N.; Chen, Z.; Jiang, B.; Sun, Y.; Yang, X.; Zhang, L. Fabrication of Meshes with Inverse Wettability Based on the TiO<sub>2</sub> Nanowires for Continuous Oil/Water Separation. *Chem. Eng. J.* **2019**, *380*, 122524. [[CrossRef](#)]
26. Su, X.J.; Li, H.Q.; Lai, X.J.; Zhang, L.; Liao, X.F.; Wang, J.; Chen, Z.H.; He, J.; Zeng, X.R. Dual-Functional Superhydrophobic Textiles with Asymmetric Roll-Down/Pinned States for Water Droplet Transportation and Oil-Water Separation. *ACS Appl. Mater. Interfaces* **2018**, *10*, 4213–4221. [[CrossRef](#)]
27. Li, Z.T.; He, F.A.; Lin, B. Preparation of Magnetic Superhydrophobic Melamine Sponge for Oil-Water Separation. *Powder Technol.* **2019**, *345*, 571–579. [[CrossRef](#)]
28. Ge, J.; Ye, Y.D.; Yao, H.B.; Zhu, X.; Wang, X.; Wu, L.; Wang, J.L.; Ding, H.; Yong, N.; He, L.H.; et al. Pumping through Porous Hydrophobic/Oleophilic Materials: An Alternative Technology for Oil Spill Remediation. *Angew. Chem. Int. Ed. Engl.* **2014**, *53*, 3612–3616. [[CrossRef](#)]
29. Dhar, M.; Das, A.; Shome, A.; Borbora, A.; Manna, U. Design of ‘Tolerant and Hard’ Superhydrophobic Coatings to Freeze Physical Deformation. *Mater. Horiz.* **2021**, *10*, 2717–2725. [[CrossRef](#)]
30. Rong, J.; Zhang, T.; Qiu, F.X.; Xu, J.C.; Zhu, Y.; Yang, D.Y.; Dai, Y.T. Design and Preparation of Efficient, Stable and Superhydrophobic Copper Foam Membrane for Selective Oil Absorption and Consecutive Oil–Water Separation. *Mater. Des.* **2018**, *142*, 83–92. [[CrossRef](#)]
31. Liang, L.; Dong, Y.; Liu, Y.; Meng, X. Modification of Polyurethane Sponge Based on the Thiol–Ene Click Reaction and Its Application for Oil/Water Separation. *Polymers* **2019**, *11*, 2072. [[CrossRef](#)]
32. Peng, M.; Zhu, Y.; Li, H.; He, K.; Zeng, G.; Chen, A.; Huang, Z.; Huang, T.; Yuan, L.; Chen, G. Synthesis and Application of Modified Commercial Sponges for Oil-Water Separation. *Chem. Eng. J.* **2019**, *373*, 213–226. [[CrossRef](#)]
33. Zeng, X.; Qian, L.; Yuan, X.; Zhou, C.; Li, Z.; Cheng, J.; Xu, S.; Wang, S.; Pi, P.; Wen, X. Inspired by *Stenocara* Beetles: From Water Collection to High-Efficiency Water-in-Oil Emulsion Separation. *ACS Nano* **2017**, *11*, 760–769. [[CrossRef](#)]
34. Zhang, W.; Shi, Z.; Zhang, F.; Liu, X.; Jin, J.; Jiang, L. Superhydrophobic and Superoleophilic PVDF Membranes for Effective Separation of Water-in-Oil Emulsions with High Flux. *Adv. Mater.* **2013**, *25*, 2071–2076. [[CrossRef](#)]
35. Yang, J.; Wang, H.; Tao, Z.; Liu, X.; Wang, Z.; Yue, R.; Cui, Z. 3D Superhydrophobic Sponge with a Novel Compression Strategy for Effective Water-In-Oil Emulsion Separation and Its Separation Mechanism. *Chem. Eng. J.* **2019**, *359*, 149–158. [[CrossRef](#)]
36. Viswanathan, P.; Johnson, D.W.; Hurley, C.; Cameron, N.R.; Battaglia, G. 3D Surface Functionalization of Emulsion-Templated Polymeric Foams. *Macromolecules* **2014**, *47*, 7091–7098. [[CrossRef](#)]
37. Moon, S.; Kim, J.Q.; Kim, B.Q.; Chae, J.; Choi, S.Q. Processable Composites with Extreme Material Capacities: Toward Designer High Internal Phase Emulsions and Foams. *Chem. Mater.* **2020**, *32*, 4838–4854. [[CrossRef](#)]
38. Li, D.; Bu, X.; Xu, Z.; Luo, Y.; Bai, H. Bioinspired Multifunctional Cellular Plastics with a Negative Poisson’s Ratio for High Energy Dissipation. *Adv. Mater.* **2020**, *32*, e2001222. [[CrossRef](#)]
39. Gui, H.; Zhang, T.; Guo, Q. Nanofibrous, Emulsion-Templated Syndiotactic Polystyrenes with Superhydrophobicity for Oil Spill Cleanup. *ACS Appl. Mater. Interfaces* **2019**, *11*, 36063–36072. [[CrossRef](#)]
40. Guan, X.; Jiang, H.; Ngai, T. Pickering High Internal Phase Emulsions Templated Super-Hydrophobic–Oleophilic Elastic Foams for Highly Efficient Oil/Water Separation. *ACS Appl. Polym. Mater.* **2020**, *2*, 5664–5673. [[CrossRef](#)]
41. Dong, B.; Wang, F.; Abadikhah, H.; Hao, L.Y.; Xu, X.; Khan, S.A.; Wang, G.; Agathopoulos, S. Simple Fabrication of Concrete with Remarkable Self-Cleaning Ability, Robust Superhydrophobicity, Tailored Porosity, and Highly Thermal and Sound Insulation. *ACS Appl. Mater. Interfaces* **2019**, *11*, 42801–42807. [[CrossRef](#)] [[PubMed](#)]
42. Huang, H.; Li, X.; Zhao, C.; Zhu, L.; Li, Y.; Wu, Y.; Li, Z. Superhydrophobic and Magnetic PS/Fe<sub>3</sub>O<sub>4</sub> Sponge for Remote Oil Removal under Magnetic Driven, Continuous Oil Collection, and Oil/Water Emulsion Separation. *J. Mater. Sci.* **2022**, *57*, 336–350. [[CrossRef](#)]
43. Azman, M.; Chungprempree, J.; Preechawong, J.; Sapsrithong, P.; Nithitanakul, M. Layer-by-Layer (LbL) Surface Augmented Modification of Poly(Styrene/Divinylbenzene)High Internal Phase Emulsion for Carbon Dioxide Capture. *Polymers* **2021**, *13*, 2247. [[CrossRef](#)] [[PubMed](#)]
44. Zhang, N.; Zhou, Y.; Zhang, Y.; Jiang, W.; Wang, T.; Fu, J. Dual-Templating Synthesis of Compressible and Superhydrophobic Spongy Polystyrene for Oil Capture. *Chem. Eng. J.* **2018**, *354*, 245–253. [[CrossRef](#)]
45. Benaddi, A.O.; Cohen, O.; Matyjaszewski, K.; Silverstein, M.S. RAFT Polymerization within High Internal Phase Emulsions: Porous Structures, Mechanical Behaviors, and Uptakes. *Polymer* **2021**, *213*, 123327. [[CrossRef](#)]
46. Deng, S.; Zhao, C.; Zhu, L.; Huang, H.; Li, Y.; Xiang, D.; Li, H.; Wu, Y.; Huang, S. Thermally Stable and Superhydrophobic Foam Prepared by High-Internal Phase Emulsion for Oil/Water Separation with Good Recycling Capacity. *J. Appl. Polym. Sci.* **2021**, *139*, 51521. [[CrossRef](#)]
47. Li, Y.; Zhang, G.; Gao, A.; Cui, J.; Zhao, S.; Yan, Y. Robust Graphene/Poly(vinyl alcohol) Janus Aerogels with a Hierarchical Architecture for Highly Efficient Switchable Separation of Oil/Water Emulsions. *ACS Appl. Mater. Interfaces* **2019**, *11*, 36638–36648. [[CrossRef](#)]
48. Zhang, N.; Zhong, S.; Zhou, X.; Jiang, W.; Wang, T.; Fu, J. Superhydrophobic P (St-DVB) Foam Prepared by the High Internal Phase Emulsion Technique for Oil Spill Recovery. *Chem. Eng. J.* **2016**, *298*, 117–124. [[CrossRef](#)]

49. Li, C.; Jin, M.; Wan, D. Evolution of a Radical-Triggered Polymerizing High Internal Phase Emulsion into an Open-Cellular Monolith. *Macromol. Chem. Phys.* **2019**, *220*, 1900216. [[CrossRef](#)]
50. Wu, H.; Shi, J.; Ning, X.; Long, Y.Z.; Zheng, J. The High Flux of Superhydrophilic-Superhydrophobic Janus Membrane of cPVA-PVDF/PMMA/GO by Layer-by-Layer Electrospinning for High Efficiency Oil-Water Separation. *Polymers* **2022**, *14*, 621. [[CrossRef](#)]
51. Zheng, Z.; Zheng, X.; Wang, H.; Du, Q. Macroporous Graphene Oxide-Polymer Composite Prepared through Pickering High Internal Phase Emulsions. *ACS Appl. Mater. Interfaces* **2013**, *5*, 7974–7982. [[CrossRef](#)] [[PubMed](#)]
52. Yu, H.; Wang, Q.; Zhao, Y.; Wang, H.; Heng, Y. A Convenient and Versatile Strategy for the Functionalization of Silica Foams Using High Internal Phase Emulsion Templates as Microreactors. *ACS Appl. Mater. Interfaces* **2020**, *12*, 14607–14619. [[CrossRef](#)] [[PubMed](#)]
53. Ye, S.; Wang, B.; Pu, Z.; Liu, T.; Feng, Y.; Han, W.; Liu, C.; Shen, C. Flexible and Robust Porous Thermoplastic Polyurethane/Reduced Graphene Oxide Monolith with Special Wettability for Continuous Oil/Water Separation in Harsh Environment. *Sep. Purif. Technol.* **2021**, *266*, 118553. [[CrossRef](#)]
54. Yu, C.; Jiang, J.E.; Liu, Y.Y.; Liu, K.; Situ, Z.Q.; Tian, L.F.; Luo, W.J.; Hong, P.Z.; Li, Y. Facile Fabrication of Compressible, Magnetic and Superhydrophobic Poly(DVB-MMA) Sponge for High-Efficiency Oil-Water Separation. *J. Mater. Sci.* **2020**, *56*, 3111–3126. [[CrossRef](#)]
55. Shi, Y.; Wang, B.; Ye, S.; Zhang, Y.; Wang, B.; Feng, Y.; Han, W.; Liu, C.; Shen, C. Magnetic, Superelastic and Superhydrophobic Porous Thermoplastic Polyurethane Monolith with Nano-Fe<sub>3</sub>O<sub>4</sub> Coating for Highly Selective and Easy-Recycling Oil/Water Separation. *Appl. Surf. Sci.* **2021**, *535*, 147690. [[CrossRef](#)]
56. Wang, J.; He, B.; Ding, Y.; Li, T.; Zhang, W.; Zhang, Y.; Liu, F.; Tang, C.Y. Beyond Superwetting Surfaces: Dual-Scale Hyperporous Membrane with Rational Wettability for “Nonfouling” Emulsion Separation via Coalescence Demulsification. *ACS Appl. Mater. Interfaces* **2021**, *13*, 4731–4739. [[CrossRef](#)]
57. Chen, C.; Liu, M.; Hou, Y.; Zhang, L.; Li, M.; Wang, D.; Fu, S. Microstructure-Controllable Nanocomplexes Bulk Possessed with Durable Superhydrophobicity. *Chem. Eng. J.* **2020**, *389*, 124420. [[CrossRef](#)]
58. Zhang, A.; Chen, M.; Du, C.; Guo, H.; Bai, H.; Li, L. Poly(dimethylsiloxane) Oil Absorbent with a Three-Dimensionally Interconnected Porous Structure and Swellable Skeleton. *ACS Appl. Mater. Interfaces* **2013**, *5*, 10201–10206. [[CrossRef](#)]
59. Wang, M.; Zhang, Z.; Wang, Y.; Zhao, X.; Yang, M.; Men, X. Durable Superwetting Materials through Layer-By-Layer Assembly: Multiple Separations Towards Water/Oil Mixtures, Water-In-Oil and Oil-In-Water Emulsions. *Colloids Surfaces A Physicochem. Eng. Asp.* **2019**, *571*, 142–150. [[CrossRef](#)]
60. Lv, Y.; Ding, Y.; Wang, J.; He, B.; Yang, S.; Pan, K.; Liu, F. Carbonaceous Microsphere/Nanofiber Composite Superhydrophilic Membrane with Enhanced Anti-adhesion Property Towards Oil and Anionic Surfactant: Membrane Fabrication and Applications. *Sep. Purif. Technol.* **2020**, *235*, 116189. [[CrossRef](#)]
61. Lv, W.Y.; Mei, Q.; Xiao, J.; Du, M.; Zheng, Q. 3D Multiscale Superhydrophilic Sponges with Delicately Designed Pore Size for Ultrafast Oil/Water Separation. *Adv. Funct. Mater.* **2017**, *27*, 1704293. [[CrossRef](#)]
62. Wang, F.; Pi, J.; Li, J.Y.; Song, F.; Feng, R.; Wang, X.L.; Wang, Y.Z. Highly-Efficient Separation of Oil and Water Enabled by a Silica Nanoparticle Coating with pH-Triggered Tunable Surface Wettability. *J. Colloid Interface Sci.* **2019**, *557*, 65–75. [[CrossRef](#)] [[PubMed](#)]